

October 31, 1983

FRA-TM-148

Transition Phase Neutronics Analysis
of an Unprotected Loss-of-Flow
Accident at EOC-4 in CRBRP

by

Ronald B. Turski

Applied Physics Division
Argonne National Laboratory
9700 South Cass Avenue
Argonne, Illinois 60439

FRA TECHNICAL MEMORANDUM NO. 148

Results reported in the FRA-TM series of memorandum frequently are preliminary and subject to revision. Consequently they should not be quoted or referenced without the author's permission.

* Work performed under the auspices of the U.S. Department of Energy.

DISCLAIMER

This report was prepared as an account of work sponsored by an agency of the United States Government. Neither the United States Government nor any agency thereof, nor any of their employees, makes any warranty, express or implied, or assumes any legal liability or responsibility for the accuracy, completeness, or usefulness of any information, apparatus, product, or process disclosed, or represents that its use would not infringe privately owned rights. Reference herein to any specific commercial product, process, or service by trade name, trademark, manufacturer, or otherwise, does not necessarily constitute or imply its endorsement, recommendation, or favoring by the United States Government or any agency thereof. The views and opinions of authors expressed herein do not necessarily state or reflect those of the United States Government or any agency thereof.

October 31, 1983

FRA-TM-148

Transition Phase Neutronics Analysis
of an Unprotected Loss-of-Flow
Accident at EOC-4 in CRBRP

by

Ronald B. Turski

Applied Physics Division
Argonne National Laboratory
9700 South Cass Avenue
Argonne, Illinois 60439

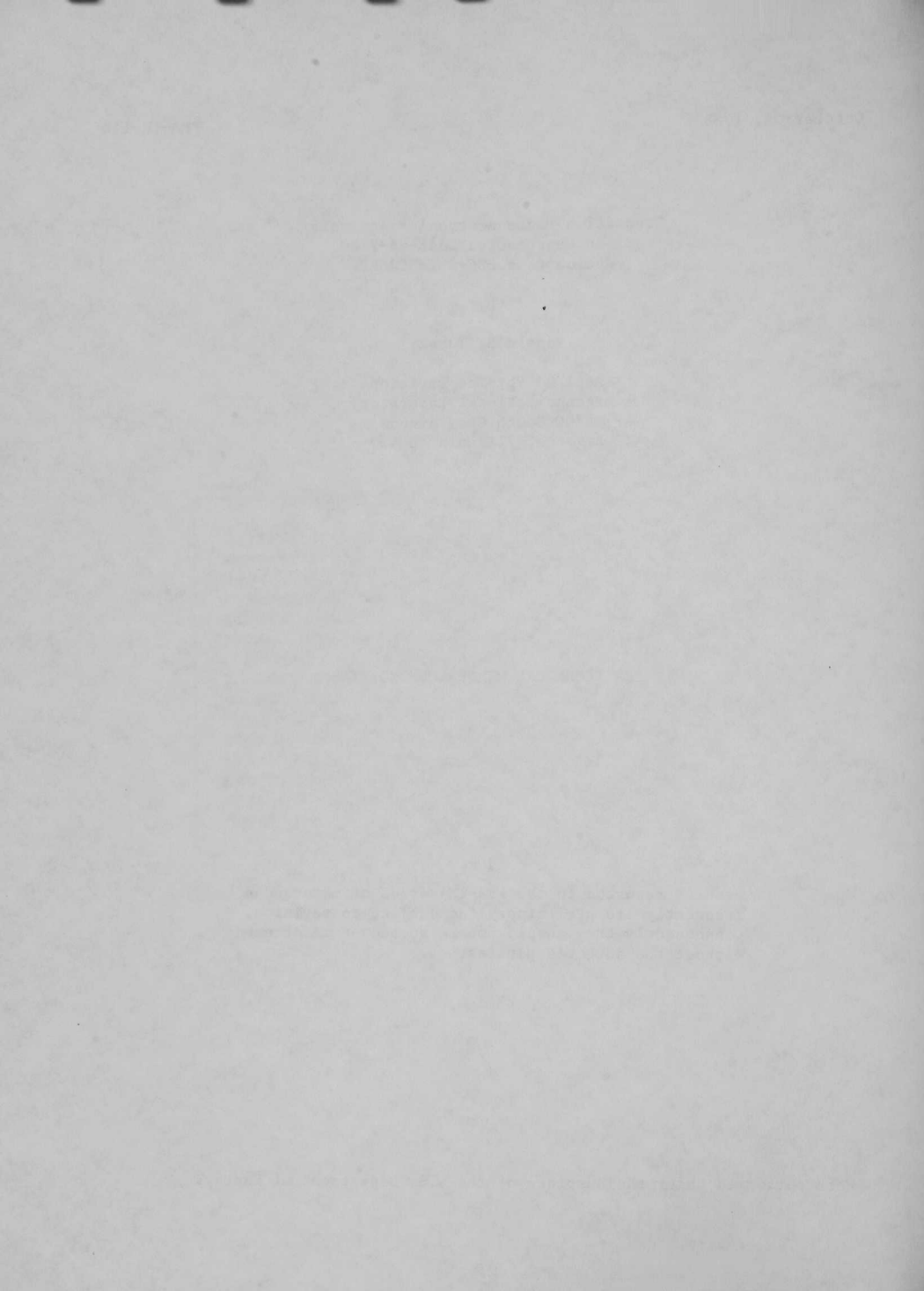
ABSTRACT

A neutronics analysis of the transition phase of an unprotected
loss-of-flow accident in CRBRP was performed by RB-TM. This study
examines the reactivity potential during the accident progression
beyond the initial phase into the transition between phase and
large scale peak power. The neutronics analysis follows as closely as
possible the best estimate description for the transition phase using
the reference data and the EOC-4 conditions. 3-D transport
theory was used to determine the degree of
reactivity for various configurations.

FRA TECHNICAL MEMORANDUM NO. 148

Results reported in the FRA-TM series of memorandum
frequently are preliminary and subject to revision.
Consequently they should not be quoted or referenced
without the author's permission.

* Work performed under the auspices of the U.S. Department of Energy.



Transition Phase Neutronics Analysis
of an Unprotected Loss-of-Flow
Accident at EOC-4 in CRBRP

by

Ronald B. Turski

Applied Physics Division
Argonne National Laboratory
9700 South Cass Avenue
Argonne, Illinois 60439

ABSTRACT

A neutronics analysis of the transition phase of an unprotected loss-of-flow accident in CRBRP was performed by AP/ANL. This study evaluates the recriticality potential during the accident progression beyond the initiating phase into the transition melt-out phase and large scale pool phase. The neutronics models follow as closely as possible the best estimate scenarios for the transition phase using the reference CRBRP PSAR design at EOC-4 conditions. S-4 transport theory with isotropic scattering was used to calculate the degree of recriticality for a wide range of disrupted core configurations.

TABLE OF CONTENTS

	<u>Page</u>
Introduction	1
Computational Methodology	1
Cross Section Processing	1
Modeling Considerations	1
Neutronics Analysis of EOC-4 Transition Phase	2
Cases 1A Through 1C	2
Case 2A	3
Case 2B	3
Cases 3A Through 3C	3
Case 4A	4
Cases 5A Through 5C	4
Cases 6A Through 6C	5
Cases 7A and 7B	5
Summary of Results	5
References	7

LIST OF TABLES

<u>No.</u>	<u>Title</u>	<u>Page</u>
I.	Group Structure for 8 and 20 Group Cross Section Libraries . . .	8
II.	Heavy Metal Mass Inventory (kg) for CRBRP EOC-4	9
III.	EOC-4 LOF Transition Phase Disruptive Core Configurations	10
IV.	Transition Phase Neutronics Calculations for CRBRP EOC-4 Core . .	11

LIST OF FIGURES

<u>No.</u>	<u>Title</u>	<u>Page</u>
1.	CRBRP EOC-4 Transition Phase Base Case	13
2.	CRBRP EOC-4 Transition Phase, Case 1A	14
3.	CRBRP EOC-4 Transition Phase, Case 1B	15
4.	CRBRP EOC-4 Transition Phase, Case 1C	16
5.	CRBRP EOC-4 Transition Phase, Case 2A	17
6.	CRBRP EOC-4 Transition Phase, Case 2B	18
7.	CRBRP EOC-4 Transition Phase, Case 3A	19
8.	CRBRP EOC-4 Transition Phase, Case 3B	20
9.	CRBRP EOC-4 Transition Phase, Case 3C	21
10.	CRBRP EOC-4 Transition Phase, Case 4A	22
11.	CRBRP EOC-4 Transition Phase, Case 5A	23
12.	CRBRP EOC-4 Transition Phase, Case 5B	24
13.	CRBRP EOC-4 Total Flux Contours for Case 5B	25
14.	CRBRP EOC-4 Transition Phase, Case 5C	26
15.	CRBRP EOC-4 Transition Phase, Case 6A	27
16.	CRBRP EOC-4 Transition Phase, Case 6B	28
17.	CRBRP EOC-4 Transition Phase, Case 6C	29
18.	CRBRP EOC-4 Transition Phase, Case 7A	30

Introduction

This report documents the neutronics analysis of the recriticality potential of the post-initiating phase of an unprotected loss-of-flow accident in CRBRP at EOC-4 (end-of-cycle 4) conditions. It also represents a continuation of neutronics analysis previously done for the transition phase of an unprotected LOF accident at BOC1 in CRBRP¹ and is based on an assessment of HCDA energetics in the CRBRP heterogeneous reactor core as reported by General Electric.²

Computational Methodology

The objective of the AP/ANL analysis of CRBRP EOC-4 transition phase has been to retain as much rigour in the computational modeling as possible while limiting computational costs. As noted in the analysis of BOC-1, the presence of large internal voids which are encountered in significantly disrupted core configurations makes the use of diffusion theory suspect. In order to adequately handle large internal voids, S-4 transport with isotropic scattering was selected for all transition phase analysis.

Cross Section Processing

The basic cross section data used for the neutronics analysis were generated from the ENDF/B-IV data files³ using the MC²-2/SDX^{4,5} code system. Specific EOC-4 compositions were used to generate EOC-4 broad group libraries. The base library of 171-groups ($\Delta u = 0.1$) was generated using a weighting spectrum from a 2040-group slowing down calculation for an appropriate Pu/U fueled LMFBF core composition.⁶ Using the fine-group base library, broad group libraries were generated for EOC-4 compositions with the SDX code. Resonance self-shielding effects were accounted for in voided and nonvoided driver, internal blanket, and radial blanket assemblies. Eight group and twenty group libraries were obtained for operating conditions (1500°K) and for an elevated temperature (3000°K). Table I shows both group structures.

Modeling Considerations

The CRBRP heterogeneous core is expected to achieve a level of permanent subcriticality in a loss-of-flow (LOF) event by virtue of fuel removal from the core even under the hypothetical assumption that both shutdown systems fail to function. Analysis performed by S. K. Rhow, et al.,² shows adequate fuel removal would occur during the melt-out period after the initiating phase of the unprotected LOF event. Based on this analysis specific cases have been defined to develop a better understanding of the neutronics behavior of disrupted core configurations.

For this study the modeling considerations for the EOC-4 LOF transition phase analysis are consistent with those used for the BOC-1 transition phase analysis. The reference CRBRP design and EOC-4 mass inventories were taken from the CRBRP PSAR⁷ and are given in Table II. The corresponding full RZ neutronics model for EOC-4 CRBRP is shown in Fig. 1. This model represents

the base case on which disrupted configuration criticality potentials are determined.

For disrupted core fuel assemblies thick steel blockages are assumed to form in the Upper Axial Blanket (UAB) and at the Lower Axial Blanket (LAB)/core interface. These blockages are assumed sufficient to prevent further fuel dispersal through the assembly. In this analysis 1/3 of the driver clad and wire wrap is projected to relocate into the UAB region contributing to a 2.2 cm thick solid steel blockage inside the hexcan at a height of 20 cm above the UAB/core interface with the remaining steel homogenized over the 17.8 cm of available UAB volume below the blockage. In addition 1/3 of the driver assembly clad and wire wrap is projected to relocate downward to form a steel blockage 3 cm thick below the lower axial blanket/core interface. The excess residual steel is homogenized with the 1/3 clad and wire wrap that remains in the core region and mixes with the molten fuel and hexcan.

The failure of the hexcan wall boundary through rupture and/or melt through is assumed to make it possible for the pressurized internal assembly pool to flow into any interstitial volume between assemblies. Vapor pressure buildup is the primary driving force for dispersal of the localized fuel-steel pools into the interstitial volume available below the core/LAB interface. This corresponds to a 19.7 in. penetration length (14 in. LAB + 5.7 in. below blanket into shield block) in 253 subassemblies with an average interassembly gap width of 0.185 in. This translates into an available interstitial volume for fuel displacement below the core plus radial blanket of 185.9 liters and if the radial reflector is included of 333.6 liters.

The overheating and melt through of the control rod hexcan wall can lead to local entry of molten fuel into the control assembly below the active absorber rod location. Downward penetration into the shield and orifice zones is unrestricted.

Neutronics Analysis of EOC-4 Transition Phase

Neutronics calculations were done for several disruptive core configurations assuming CRBRP EOC-4 unprotected LOF transition phase conditions. A brief description of each configuration with respect to degree and location of fuel removal is given in Table III. The base case represents the CRBRP at EOC-4 under operating conditions. The CRBRP EOC4 fuel inventories are taken from the CRBRP PSAR.

Cases 1A Through 1C

The initial disrupted configuration of the transition phase, case 1A, as shown in Fig. 2 represents the condition in which the driver fuel is assumed to slump, melt, and mix with the available steel to form a single pool, single phase, fully dense composition. The internal blankets, control assemblies, and radial blanket assemblies remain intact. Steel blockages are assumed to form in the driver assemblies at 20 cm above the UAB/core interface and at the LAB/core interface. Of the 40% of the slumped driver fuel 10% flows through the interstitial gaps to below the core, lower axial blanket, and lower radial blankets, and 30% into the lower radial shield. All fission products in molten

fuel are assumed to vent from the system. This is a conservative assumption that holds for all the following cases. For a 40% removal of fuel from the active core region the recriticality potential is -5.82% . A description of the recriticality potential for all cases is given in Table IV.

Case 1B shown in Fig. 3 is the same as 1A except that of the 50% of the driver fuel removed 10% is relocated to below the core into the lower axial and radial blankets, and 40% into the radial shield. The removal of an additional 10% of driver fuel reduces the recriticality potential to -22.96% . Case 1C shown in Fig. 4 is the same as 1A except that only 30% of the driver fuel is relocated with 10% moving to below the core and into the lower axial and radial blankets and 20% moving to the lower radial shield. The recriticality potential increases to $+8.62\%$.

Case 2A

In case 2A the upper axial blanket fuel plus clad and wire wrap fall and mix with the molten driver fuel forming a single level, single phase pool, see Fig. 5. The internal blankets, control assemblies, and radial blankets remain intact, while 20% of the original driver fuel is relocated to below the core with 6% in the lower axial and radial blankets and 14% in the radial shield regions. The addition of axial blanket fuel and structure to the molten driver pool acts as a diluent. The resulting system is -12.46% subcritical.

Case 2B

In case 2B the internal blankets, control assemblies, and 1st row of the radial blanket melt and mix with the driver fuel. Thirty percent of the driver fuel is relocated, of which 7% flows to below the core into the lower axial and radial blankets, 8% flows to below the control assemblies, and 15% flows into the lower radial shield. This configuration is shown in Fig. 6. The slumping of the internal blankets has a positive effect on recriticality but is more than compensated for by the diluent effect of the mixing with the control assemblies, driver fuel, and radial blanket. The net effect is a -5.12% subcritical system.

Cases 3A Through 3C

In case 3A 50% of the driver fuel is relocated to below the core with 10% in the lower axial and radial blankets, 8% below the control assemblies and 32% in the lower radial shield. The internal blankets and control assembly channels melt and mix with the driver fuel, see Fig. 7. The steel content of the core is reduced by 50% with the displaced steel mixing uniformly with the displaced core material. The resulting configuration is -11.28% subcritical.

Case 3B is similar to 3A except the original steel content of the core, internal blankets, and control assemblies separates from the fuel and forms a pool of molten steel above a pool of fuel. This acts as a strong reflector and increases the criticality to $+8.15\%$. This configuration is shown in Fig. 8.

In case 3C the upper axial blanket, cladding and wire wrap fall and mix with the core pool as described for case 3B. The steel and fuel continue to separate forming separate pools but the increased dilution caused by the addition of upper axial blanket fuel cause the recriticality to decrease to -8.57\$, see Fig. 9.

Case 4A

Case 4A is similar to case 1C in that 30% of the driver fuel is removed to below the core, with 10% in the lower axial and radial blankets, and 20% in the lower radial shield (20%); while the internal blankets and control assemblies remain intact. But, an additional 19% of the driver fuel is relocated to in-between the internal blanket rods. This configuration is shown in Fig. 10. The relocation of fuel from a high worth region to a lower worth region reduces the criticality to -0.91\$.

Cases 5A Through 5C

Case 5A is similar to case 1C in that 30% of the driver fuel is relocated to below the core, with 10% in the lower axial and radial blankets and 20% in the lower radial shield. The internal blankets and control assemblies are intact but the slumped core pool is in a state of boilup with a uniform void profile. A uniform void profile results in the remaining (70%) driver fuel and structure to be uniformly distributed throughout the available driver volume. This substantial dilution of fuel leads to a -26.20\$ subcritical condition. This configuration is shown in Fig. 11.

The extreme sensitivity of recriticality to configuration is apparent in case 5B. This case is similar to 5A except that the core pool experiences boil up with a linear void profile rather than a uniform void profile, see Fig. 12. A linear void profile is described as a 15 cm thick single-phase layer at the bottom of the pool with the remainder of the core material distributed with a uniformly increasing void fraction (i.e. 20%, 40%, 60%, 80%, 100% void). A linear void profile leads to a supercritical +0.60\$ condition. The change in configuration, from a no boilup single phase core to boilup with a linear void profile, to boilup with a uniform void profile with all other factors remaining constant, gives a shift in criticality of from +8.62\$ (1C) to +0.60\$ (5B) to -26.20\$ (5A). This is an extremely large change considering the fact that the total mass of fuel in the core region remains the same. Another interesting occurrence can be seen in Fig. 13. This figure shows the total flux contours for case 5B. The peak flux occurs in regions 6b which have a lower density of fuel than regions 6a. The movement of fuel from region 6a to the lower part of 6b would be a movement from a lower worth region to a higher worth region and would result in a more critical configuration. In general, to a first order approximation, the peak flux occurs at the center of mass for the active core zone. This implies that with less fuel removal to below the core and with a thinner fully dense single phase layer the peak flux position could be significantly moved into the less dense fuel zones. This makes the evaluation a recriticality potential very sensitive boilup scenario and selected void profiles.

Case 5C is similar to 5B except that only the inner core zones experience boilup with a linear void profile. This configuration is shown in Fig. 14. The boilup of the inner core zones gives a criticality of +7.64\$. This is only slightly less than the nonboilup condition and results from reduced leakage out of the inner core zones and the relatively smaller mass of fuel in the inner core zones when compared to that of the outer core zones.

Cases 6A Through 6C

These cases also test the criticality sensitivity to boilup. In case 6A there is no fuel removal from the core. The internal blankets and control assemblies are intact. The outer core is fully boiled up with a uniform void fraction and the two inner pools (originally fully boiled up) are compacted with a 10 cm single-phase layer at the bottom and a void space at the top. This configuration is shown in Fig. 15. The criticality is +11.66\$.

Case 6B shown in Fig. 16 is the same as 6A except that the depth of the single-phase layer in the inner pools is 20 cm. The increase in fuel compaction leads to a slightly more critical condition of +12.54\$.

Likewise case 6C is the same as 6A except that the depth of the single-phase pool layer is 30 cm. This configuration is shown in Fig. 17 and has a criticality condition of +14.20\$.

Cases 7A and 7B

In case 7A 50% of the driver cladding and wire wrap are relocated to the UAB and the remaining 50% to the LAB regions. All driver fuel, remaining hexcan steel internal blankets and control assemblies are homogenized forming a single-phase pool. No control remains in the core and all core fission products are neglected. This configuration is shown in Fig. 18 and has a criticality condition of +50.60\$.

In case 7B the configuration is the same as 7A except that the core fission products are included in the single phase pool. This results in a reduction in criticality to +44.61\$.

Summary of Results

A special effort was made in this analysis to be as rigorous as possible in the modeling. In order to minimize the errors introduced by complex configurations and streaming paths S-4 transport calculations were used and special care was taken to insure that fuel masses were conserved when moved from region to region. In general this analysis reconfirms observations made in the transition phase neutronics analysis at BOC-1 for an unprotected LOF in CRBRP.¹ The removal of an adequate amount of fuel to the available interstitial volumes below the core and core periphery can result in a subcritical condition. For EOC-4 conditions the absolute amount of fuel removed to insure subcriticality is slightly less (36%-40%) than what was needed for subcriticality in BOC-1 (approximately 44%). The reason for this is that there is a general shift in fissile inventory from the driver regions to the internal

blanket regions for EOC-4. This results in a lowering of the fissile inventory in driver regions of EOC-4 when compared with BOC-1 and hence a lessening of the amount of fuel needed to be removed to achieve subcriticality.

Similar to what was seen for BOC-1 analysis the recriticality potential for EOC-4 conditions is very sensitive to the actual configuration, boilup scenario and void profile. Even with similar amounts of fissile material within the core boundaries large variations in criticality are obtained with variations in configuration.

References

1. R. B. Turski, "Transition Phase Neutronics Analysis of an Unprotected Loss-of-Flow Accident in CRBRP," FRA-TM-147, May 20, 1983.
2. S. K. Rhow, et al., "An Assessment of HCDA Energetics in CRBRP Heterogeneous Reactor Core," CRBRP-GEFR-00523, December 1981.
3. ENDF/B Summary Documentation, BNL-NCS-17541 (ENDF 201), 2nd Edition (ENDF/B-IV), compiled by D. Garber, available from National Nuclear Data Center, Brookhaven National Laboratory, Upton, New York, October 1975.
4. H. Henryson II, B. J. Toppel, and C. G. Stenberg, "MC²-2: A Code to Calculate Fast Neutron Spectra and Multigroup Cross Sections," Argonne National Laboratory, ANL-8144, June 1976.
5. B. J. Toppel, H. Henryson II, and C. G. Stenberg, "ETOE-2/MC-2/SDX Multigroup Cross Section Processing," Proceedings of Seminar-Workshop on Multigroup Cross Sections, March 14-16, 1978, Radiation Shielding Information Center, Oak Ridge, Tennessee.
6. C. E. Till, et al., "Fast Breeder Reactor Studies," Argonne National Laboratory, ANL-80-40, July 1980.
7. CRBRP Preliminary Safety Analysis Report, Project Management Corporation, Docket No. 50-537.

TABLE I. Group Structure for 8 and 20 Group Cross Section Libraries

Broad Group Energy, eV	20 Group Library	8 Group Library
1.0000×10^7	1	1
3.6788×10^6	2	
2.2313×10^6	3	
1.3534×10^6	4	2
8.2085×10^5	5	
4.9787×10^5	6	3
3.0197×10^5	7	
1.8316×10^5	8	4
1.1109×10^5	9	
6.7380×10^4	10	5
4.0868×10^4	11	
2.4788×10^4	12	6
1.5034×10^4	13	
9.1188×10^3	14	7
5.5309×10^3	15	
3.3546×10^3	16	8
2.0347×10^3	17	
1.2341×10^3	18	
4.5400×10^2	19	
6.1442×10^1	20	

TABLE II. Heavy Metal^a Mass Inventory (kg) for CRBRP EOC-4

	Driver	Inner Blankets (1)	Radial Blanket (1)	Axial Blankets
²³⁹ Pu	1216.0	206.8	285.6	56.1
²⁴⁰ Pu	273.5	8.0	11.3	1.2
²⁴¹ Pu	32.7	-	-	-
²⁴² Pu	5.2	-	-	-
²³⁵ U	5.4	11.6	21.3	7.8
²³⁸ U	3421.0	7381.0	12936.0	4314.0
Fission Products	414.2	55.2	55.7	6.8
Total Heavy Metal	5368.0	7662.6	13309.9	4385.9

^aHeavy metal excludes oxygen.

(1) Includes axial extensions.

TABLE-III. EOC-4 LOF Transition Phase Disruptive Core Configurations

Configurations	1A-C	2A	2B	3A-B	3C	4A	5A-C	6A-C	7A-B
Fraction of Fuel Removed from Core, %	30-50	20	30	50	50	30	30	0	0
Condition of Fuel in Core	Single ϕ ⁴	Single ϕ	Single ϕ	Single ϕ ¹	Single ϕ	Single ϕ	Boilup	Boilup	Single ϕ
Condition of Internal Blankets	Intact	Intact	Mixed with fuel	Mixed with fuel	Mixed with fuel	Intact ²	Intact	Intact	Mixed with fuel
Condition of Control Assemblies	Intact	Intact	Mixed with fuel	Mixed with fuel	Mixed with fuel	Intact	Intact	Intact	Mixed with fuel
Conditions of 1st Row Radial Blanket	Intact	Intact	Mixed with fuel	Intact	Intact	Intact	Intact	Intact	Mixed with fuel
Conditions of Upper Axial Blanket	Intact	Falls and mixes with core	Intact	Intact	Falls and mixes with core	Intact	Intact	Intact	Intact ³
Location of Fuel Removed from Core, %									
Gaps between RS S/A	20-40	14	15	32	32	20	20	-	-
Gaps below core and RB	10	6	7	10	10	10	10	-	-
Control assemblies	-	-	8	8	8	-	-	-	-

¹Steel content in core reduced 50% in 3A and entire steel content of core is segregated to top of pool in 3B.

²19% single ϕ pool mixture is frozen between IB rods in core region.

³Cladding steel relocated to UAB (50%) and LAB (50%).

⁴Single phase mixture.

TABLE IV. Transition Phase Neutronics Calculations
for CRBRP EOC-4 Core

Configuration		k_{eff}	ΔK $\rho(\%)$
Base Model	CRBRP EOC-4	0.98387	-
1A	CRBRP EOC-4 compositions with 40% of the slumped driver fuel removed to the interstitial gaps below the core, RB and RS assemblies. All core fission products are removed (a conservative assumption that holds for all following cases).	0.96409	-0.01978 -5.82%
1B	Same as 1A except that 50% of driver fuel is relocated.	0.90580	-0.07807 -22.96%
1C	Same as 1A except that 30% of driver fuel is relocated.	1.01316	+0.02929 +8.62%
2A	The upper axial blanket falls and mixes with the core fuel. 20% of the total driver fuel is relocated to RS (14%) and below core gaps (6%).	0.94150	-0.04237 -12.46%
2B	The internal blankets, control rods, and 1st row of radial blanket are mixed with core fuel with 30% of the core fuel relocated to the RS (15%), below core gaps (7%) and control assemblies (8%).	0.96645	-0.01742 -5.12%
3A	Internal blankets and control rods mix with fuel with 50% of driver fuel relocated to RS, below core and RB and control assemblies. Steel content in core is reduced by 50%.	0.94552	-0.03835 -11.28%
3B	Same as 3A except that entire initial core steel content is segregated to top of pool.	1.01157	+0.02770 +8.15%
3C	Same as 3B except that UAB is mixed with fuel remaining in core region.	0.95472	-0.02915 -8.57%
4A	30% of driver fuel relocated to RS (20%), and below core (10%) with an additional (19%) of driver fuel relocated to between IB rods in core region.	0.98077	-0.00310 -0.91%

TABLE IV. Transition Phase Neutronics Calculations
for CRBRP EOC-4 Core (Cont'd)

Configuration		k_{eff}	ΔK $\rho(\%)$
Base Model			
5A	Same as 1C except that pool is boiled up with a uniform void fraction.	0.89477	-0.08910 -26.20%
5B	Same as 5A except that pool is boiled up with a linear void profile with a 15 cm single-phase layer at the bottom of the pool.	0.98590	+0.00203 +0.60%
5C	Same as 5A except that only the two inner pools are boiled up.	1.00985	+0.02598 +7.64%
6A	The outer core is fully boiled up with a uniform void fraction and the two inner pools (originally fully boiled up) are compacted with a 10 cm single phase layer at the bottom and a void space at the top. No fuel removal from the core has occurred.	1.02352	+0.03965 +11.66%
6B	Same as case 6A except the depth of the single-phase layer in the inner pools is 20 cm.	1.02650	+0.04264 +12.54%
6C	Same as case 6A except the depth of the single-phase layer in the inner pools is 30 cm.	1.03215	+0.04828 +14.20%
7A	Cladding steel relocated to UAB (50%) and LAB (50%) regions. All driver fuel, hexcan steel and IB are homogenized forming a single-phase pool. No control remains in the core and all core fission products are neglected.	1.15591	+0.17204 +50.60%
7B	Same as 7A except all core fission products are included.	1.13556	+0.15169 +44.61%

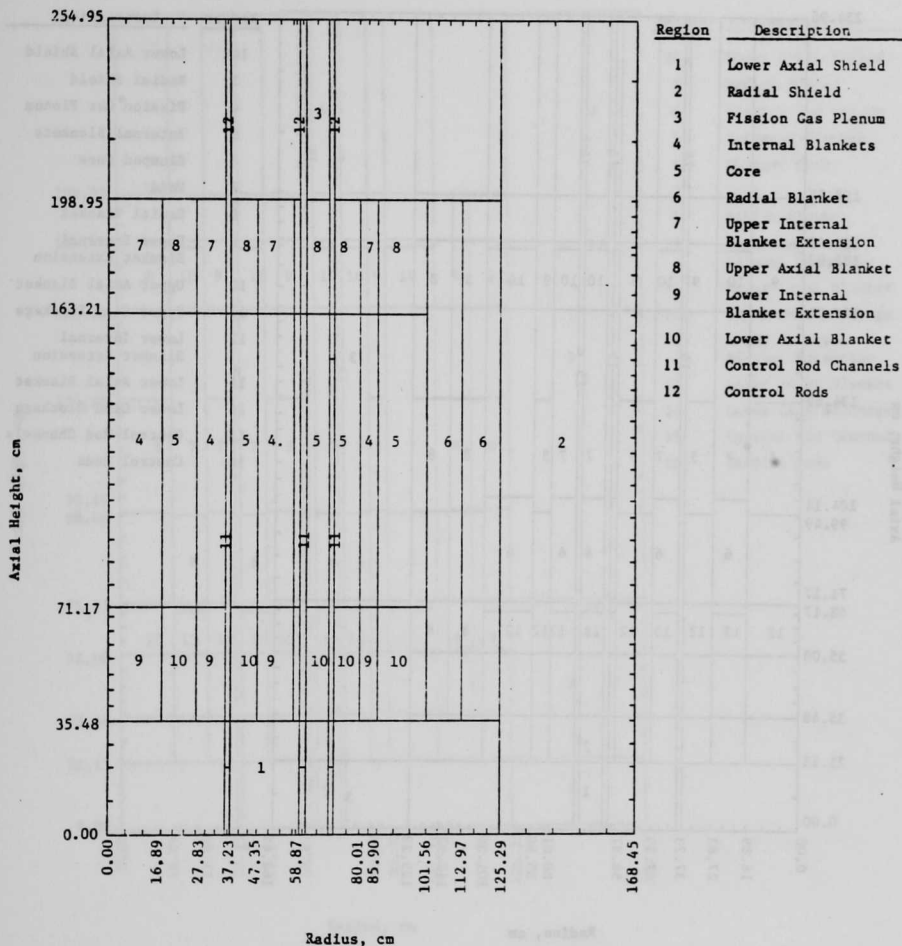


Fig. 1. CRBRP EOC-4 Transition Phase Base Case

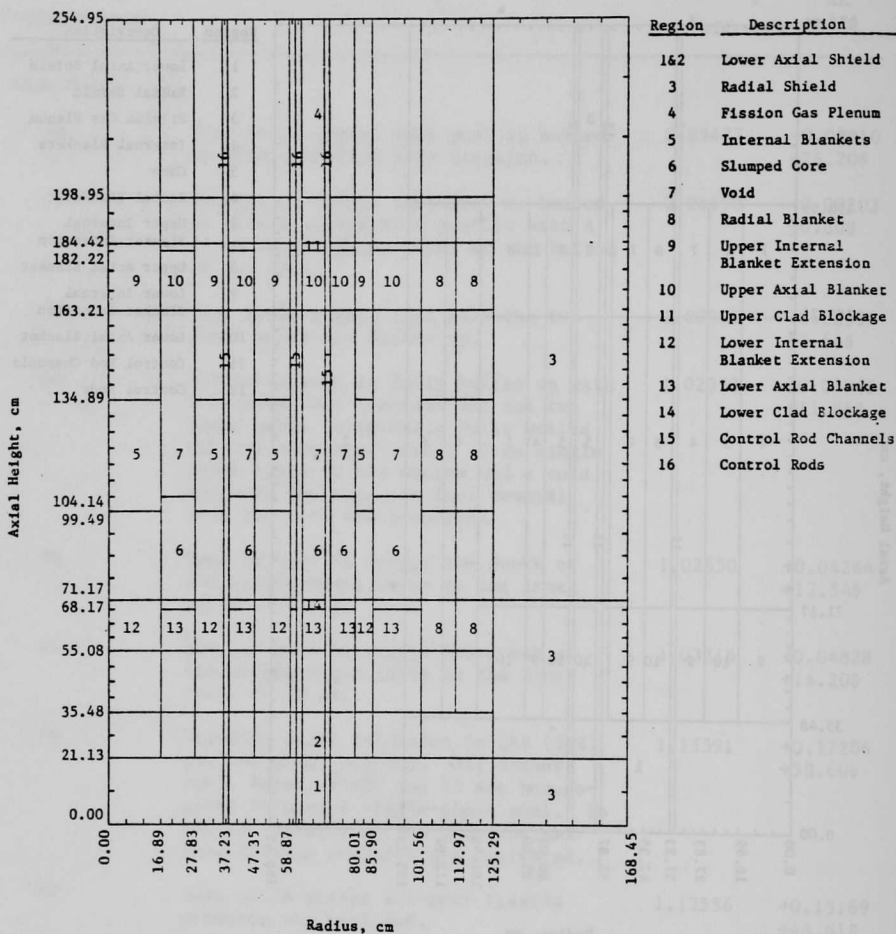


Fig. 2. CRBRP EOC-4 Transition Phase, Case 1A

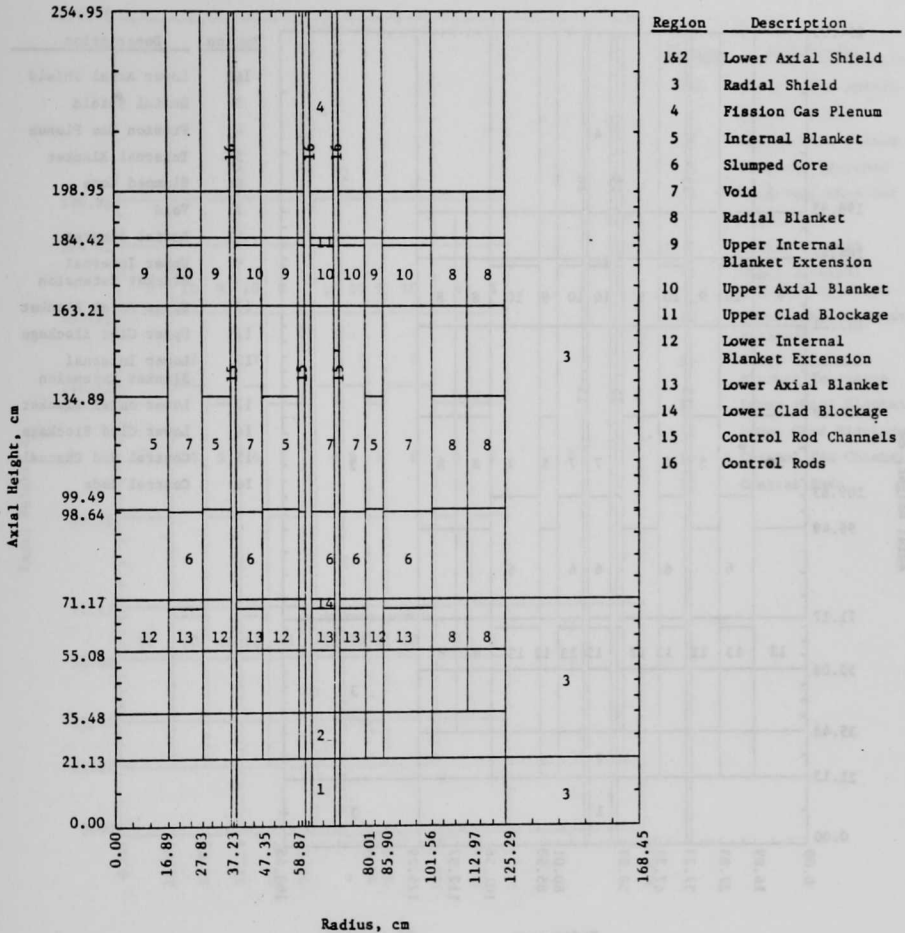


Fig. 3. CRBRP EOC-4 Transition Phase, Case 1B

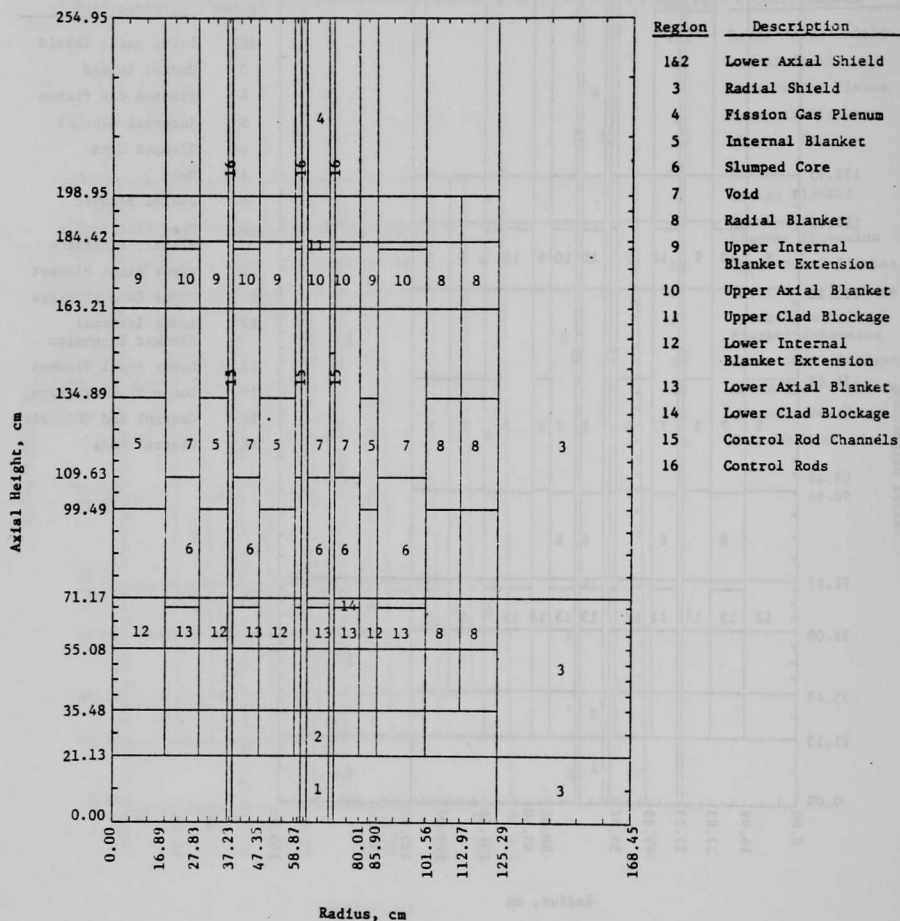


Fig. 4. CRBRP EOC-4 Transition Phase, Case 1C

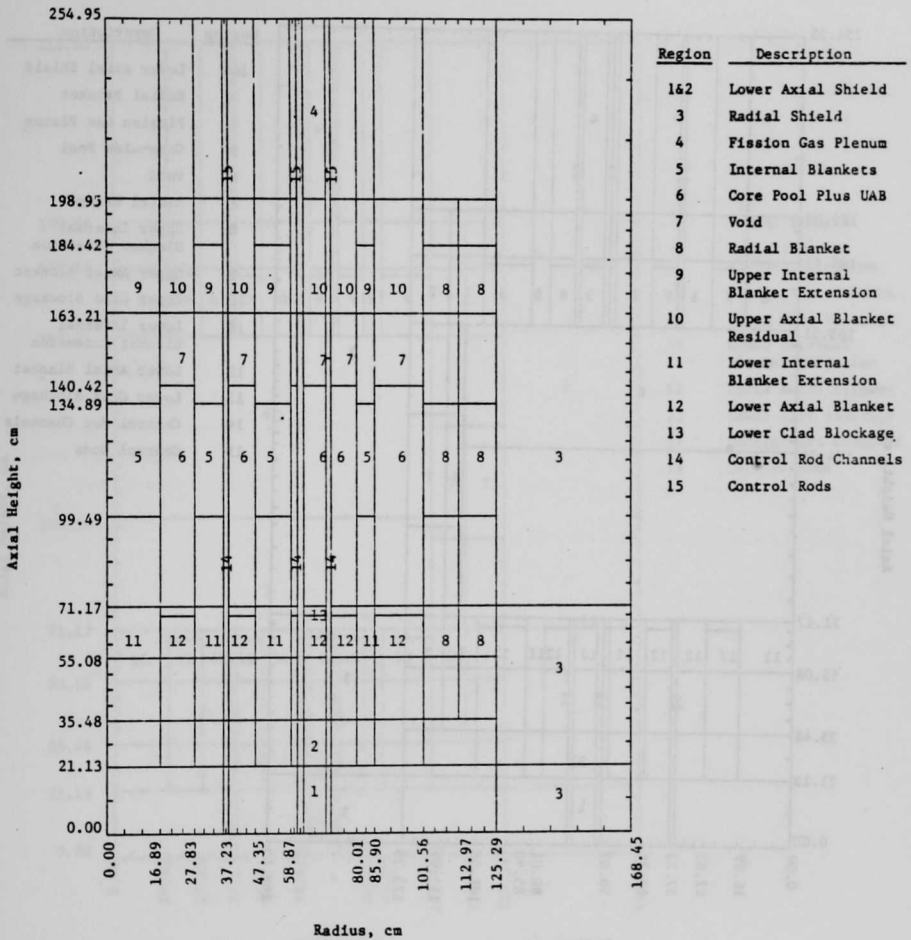


Fig. 5. CRBRP EOC-4 Transition Phase, Case 2A

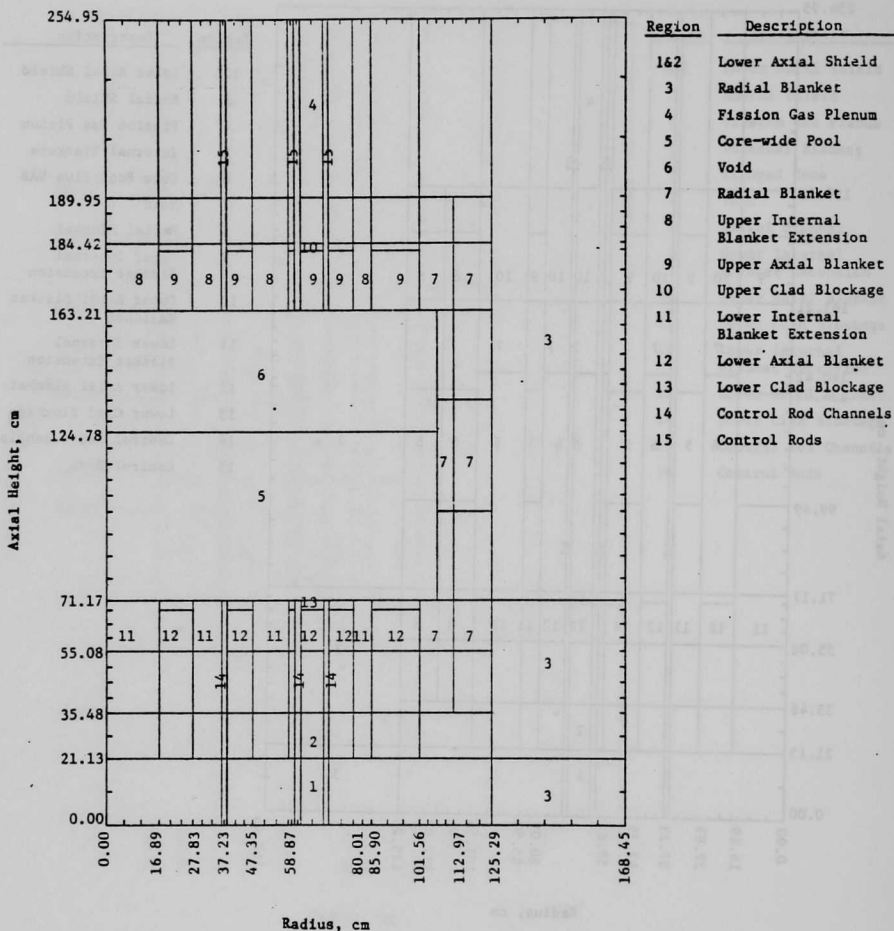


Fig. 6. CRBRP EOC-4 Transition Phase, Case 2B

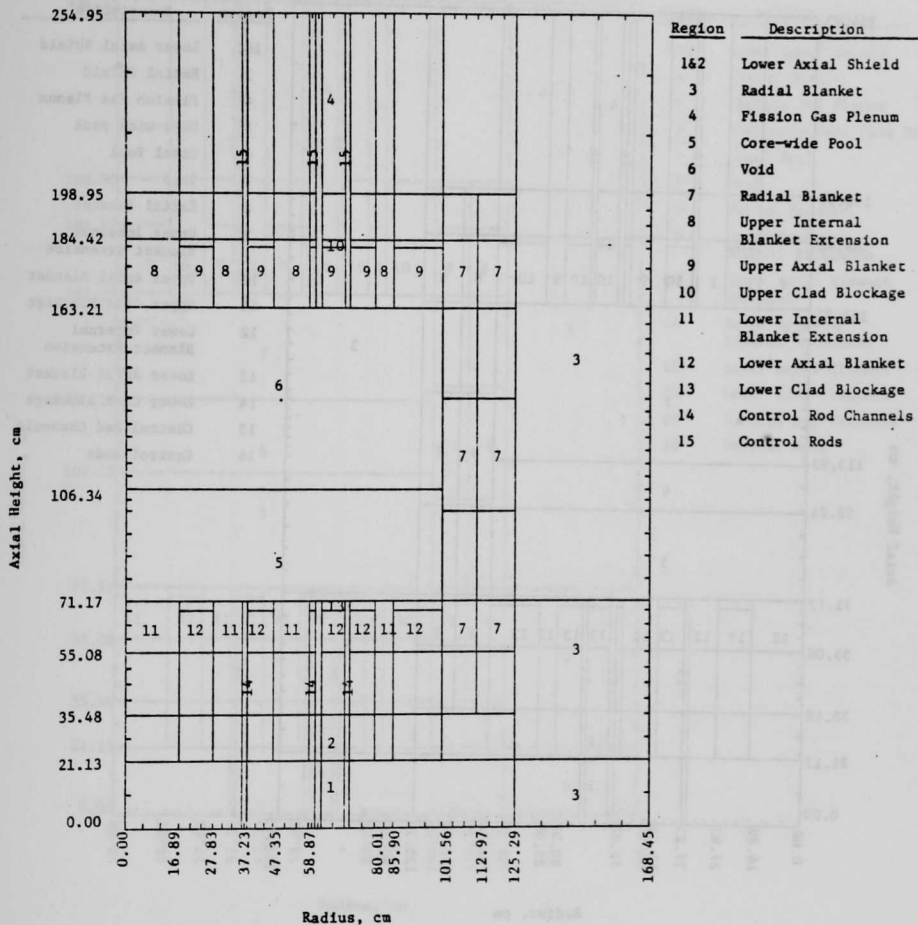


Fig. 7. CRBRP EOC-4 Transition Phase, Case 3A

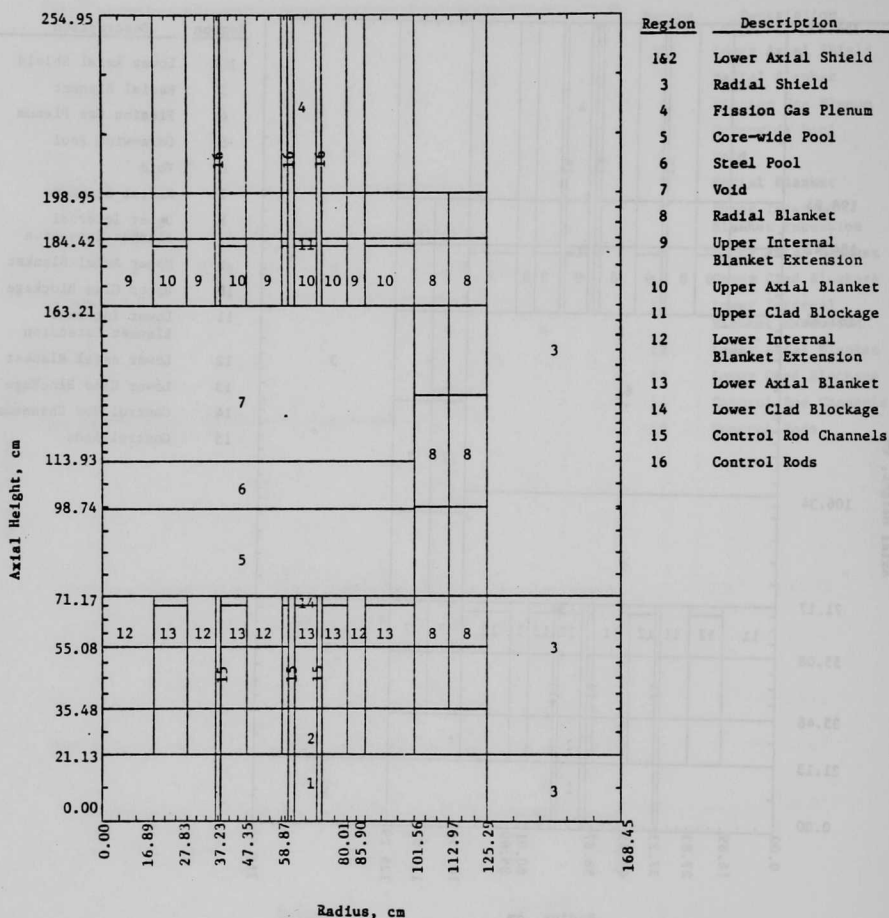


Fig. 8. CRBRP EOC-4 Transition Phase, Case 3B

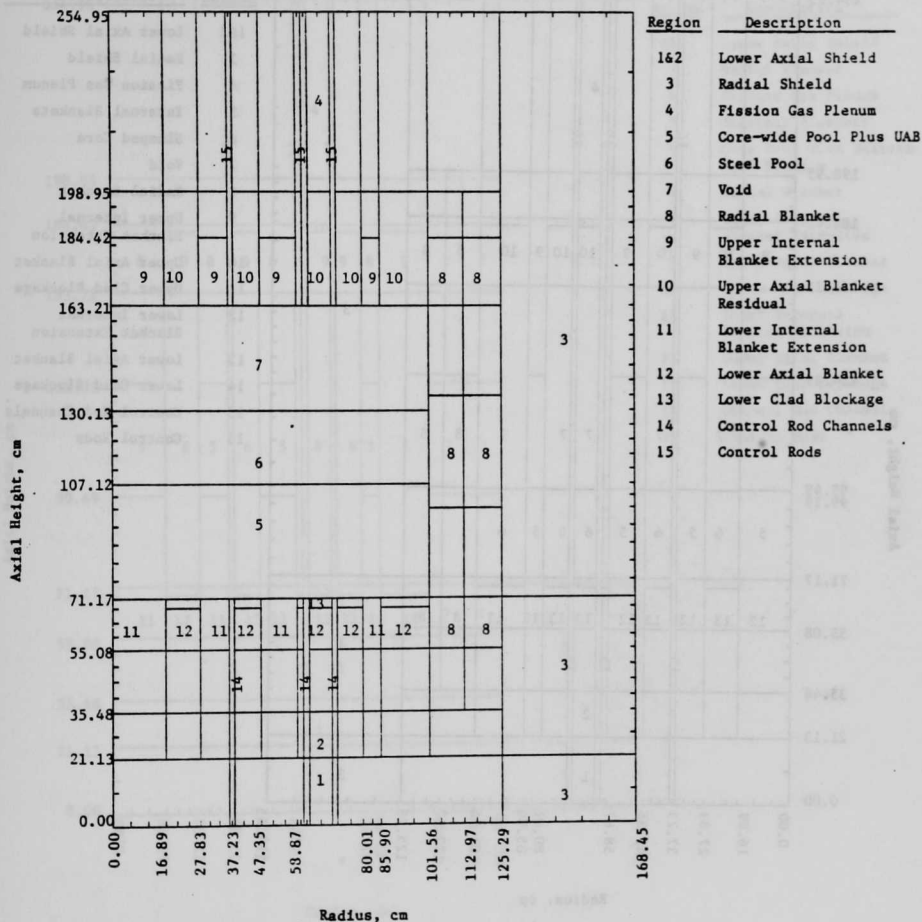


Fig. 9. CRBRP EOC-4 Transition Phase, Case 3C

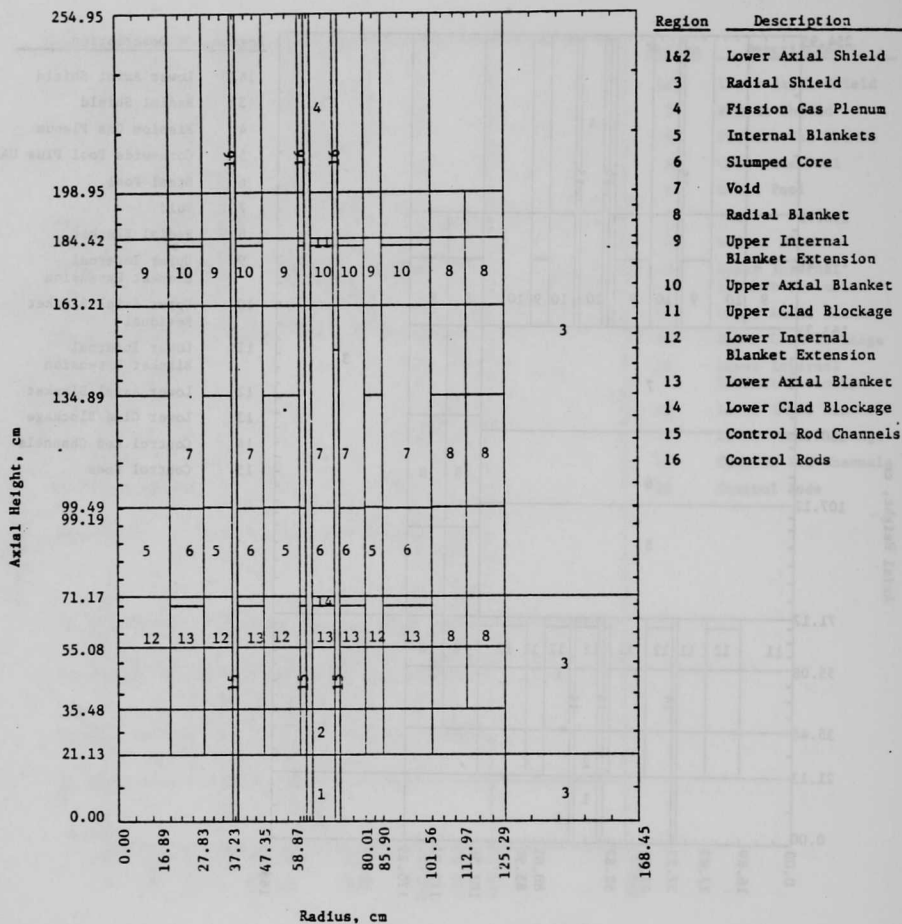


Fig. 10. CRBRP EOC-4 Transition Phase, Case 4A

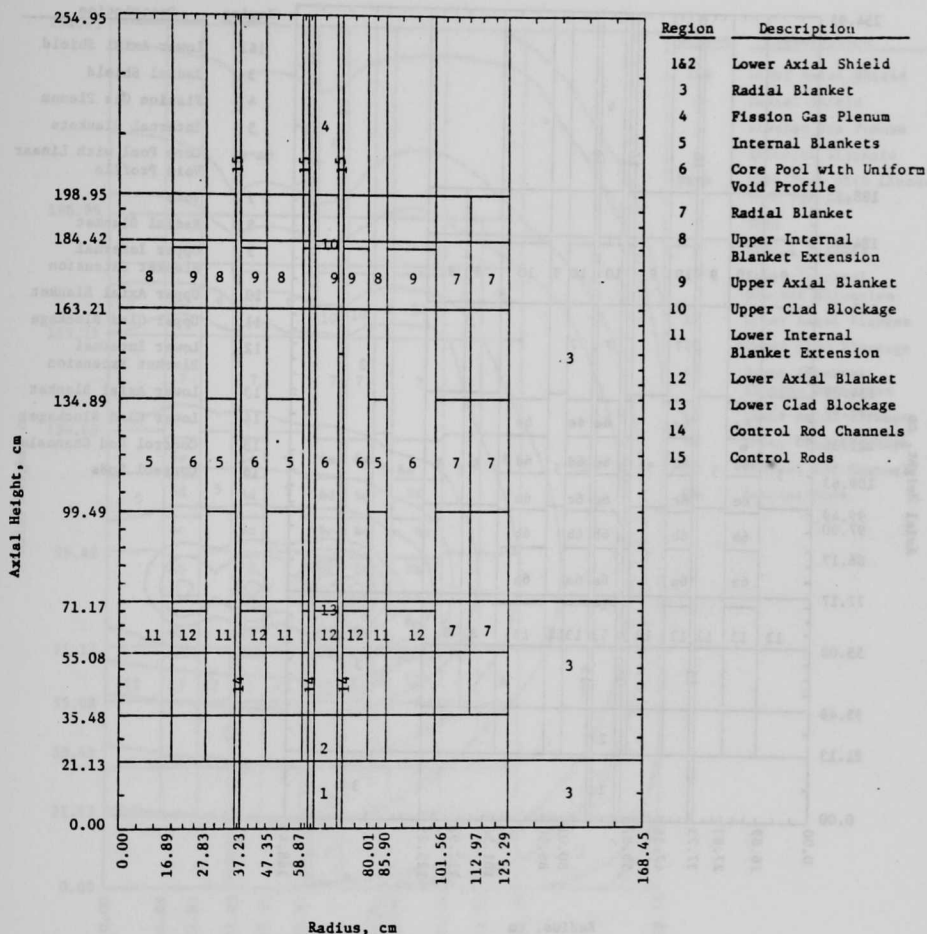


Fig. 11. CRBRP EOC-4 Transition Phase, Case 5A

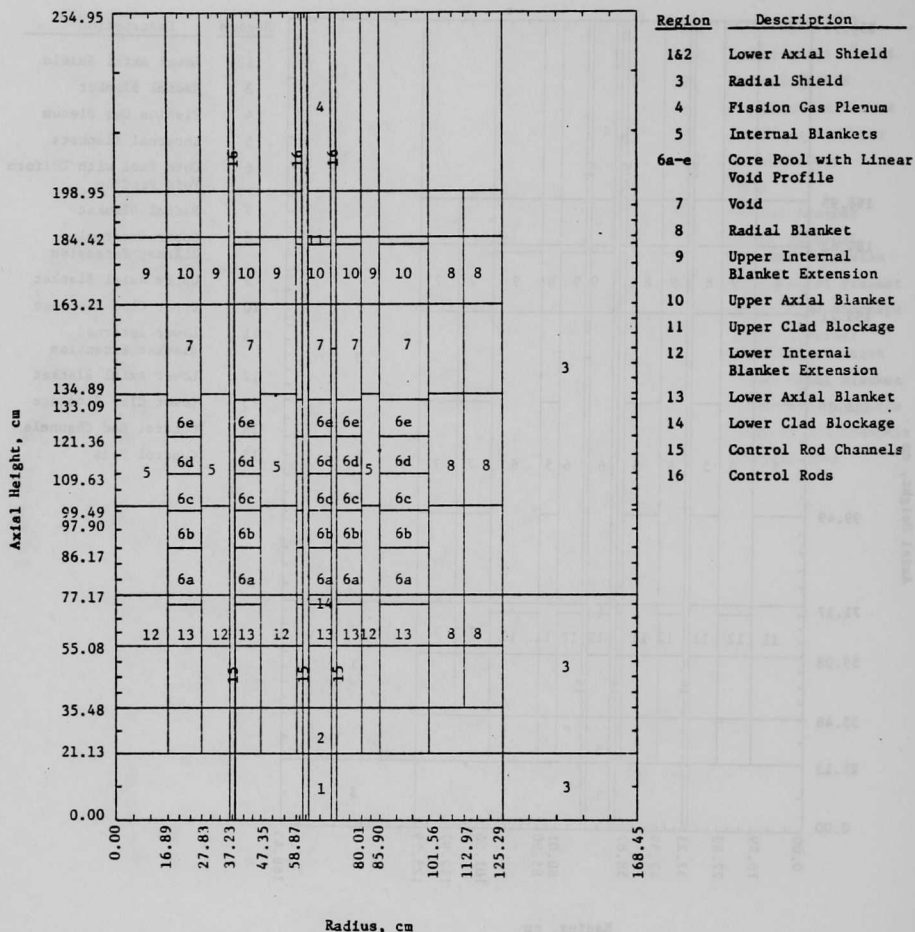


Fig. 12. CRBRP EOC-4 Transition Phase, Case 5B

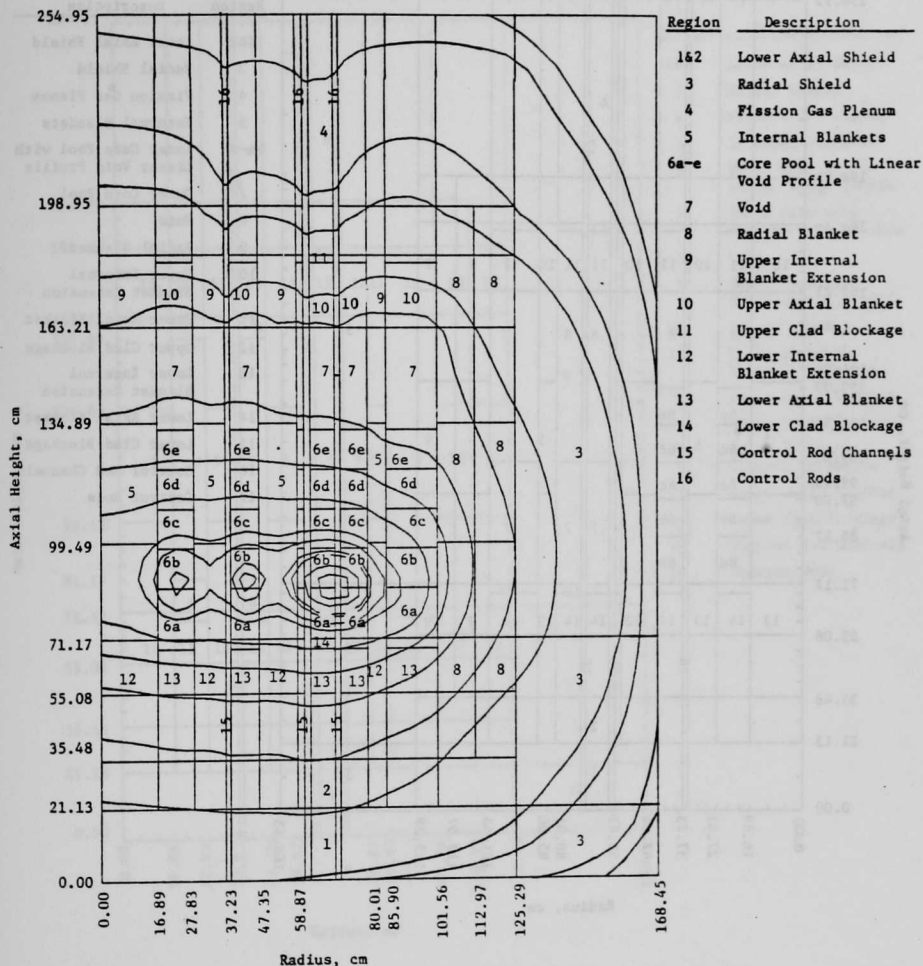


Fig. 13. CRBRP EOC-4 Total Flux Contours for Case 5B

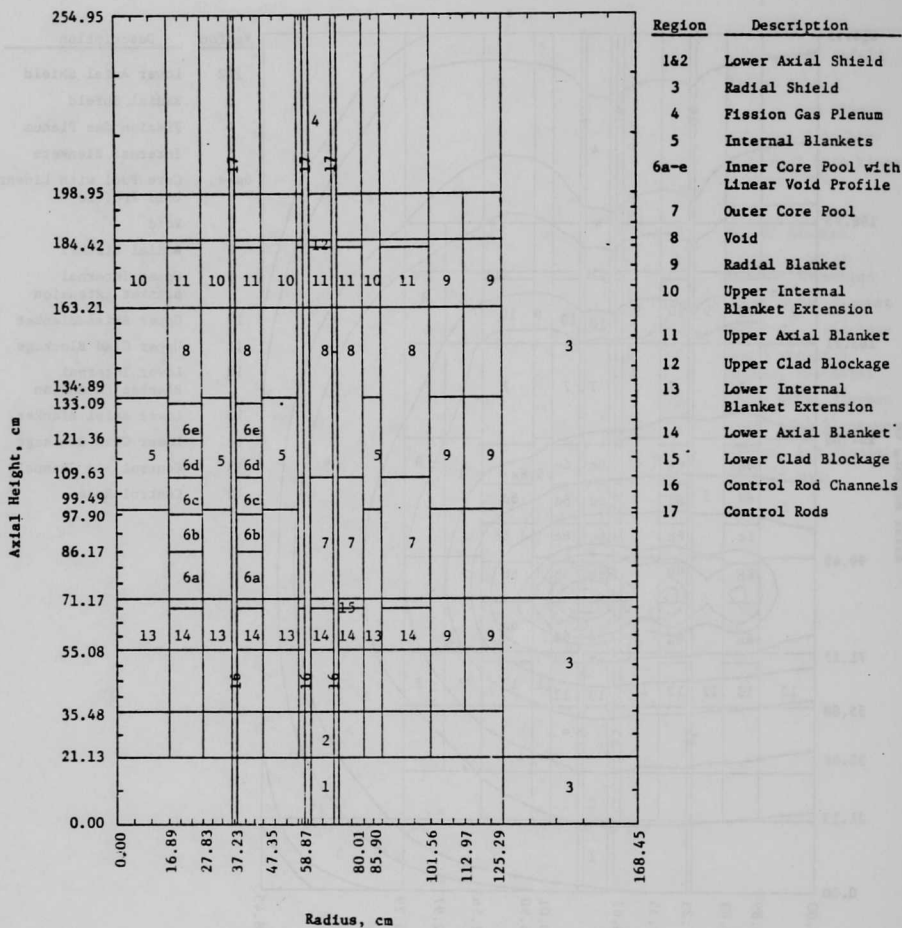


Fig. 14. CRBRP EOC-4 Transition Phase, Case 5C

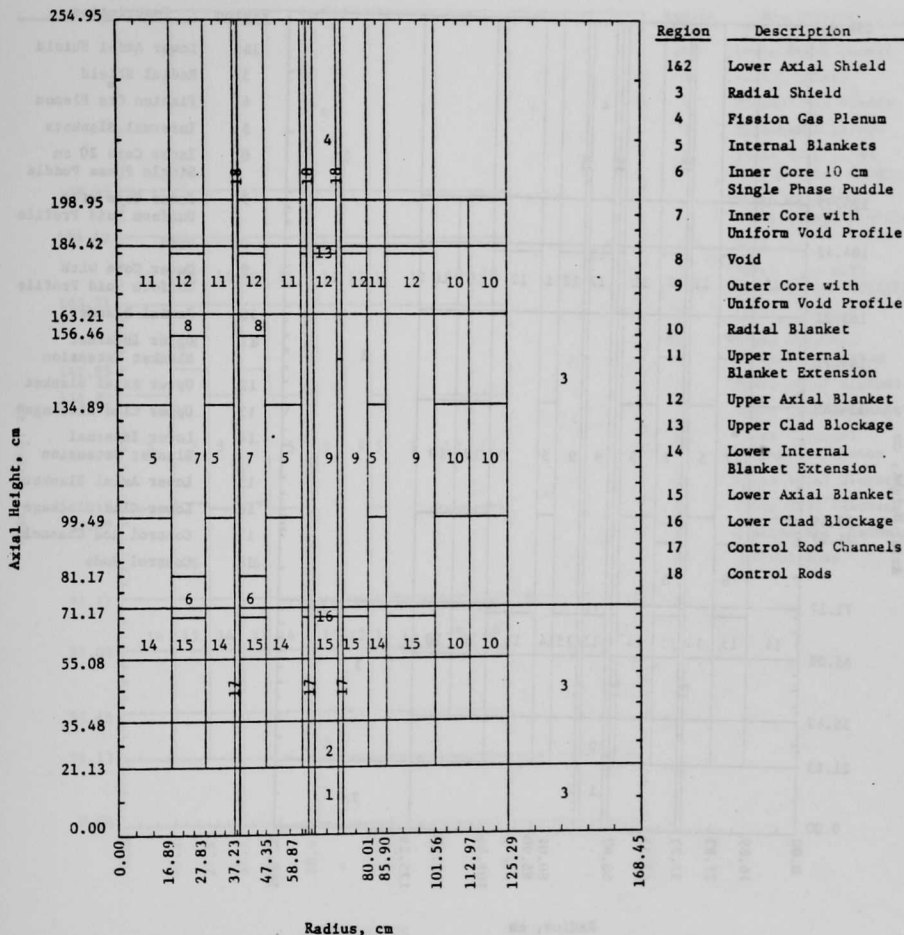


Fig. 15. CRBRP EOC-4 Transition Phase, Case 6A

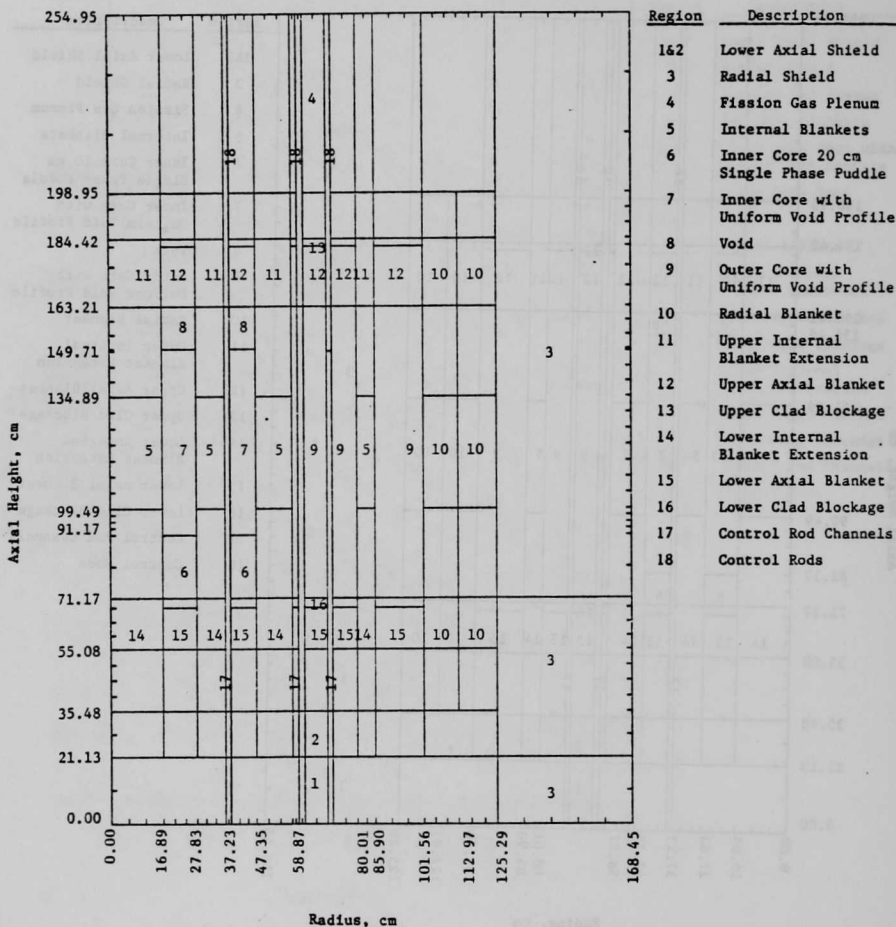


Fig. 16. CRBRP EOC-4 Transition Phase, Case 6B

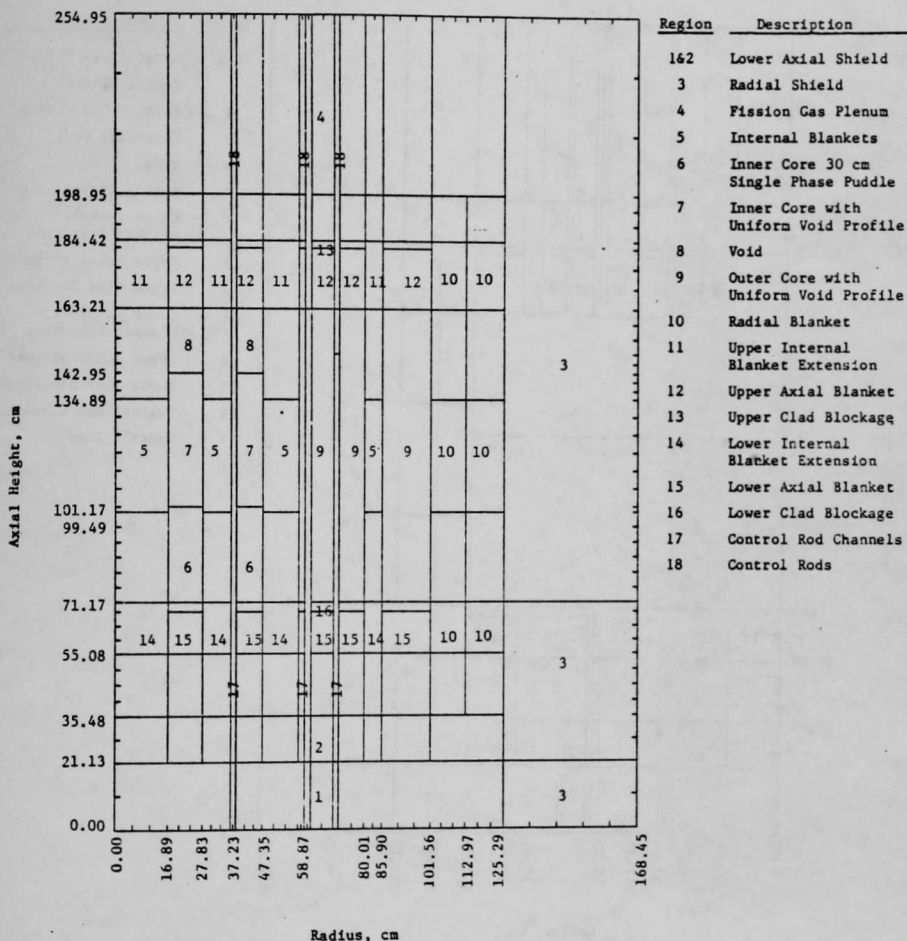


Fig. 17. CRBRP EOC-4 Transition Phase, Case 6C

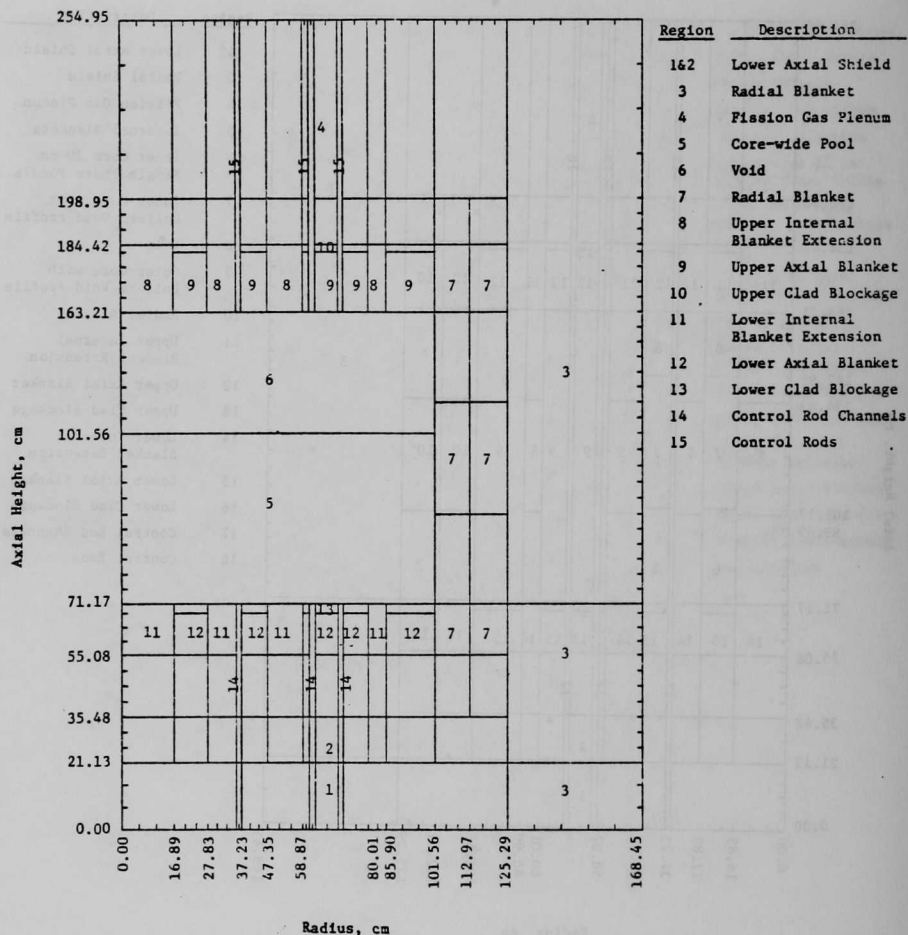


Fig. 18. CRBRP EOC-4 Transition Phase, Case 7A

9 4441 0001013 0

